



## Patient-derived induced pluripotent stem cells to study non-canonical splicing variants associated with Hypertrophic Cardiomyopathy

Joanna Jager<sup>a,1</sup>, Marta Ribeiro<sup>b,c,1</sup>, Marta Furtado<sup>d</sup>, Teresa Carvalho<sup>d</sup>, Petros Syrris<sup>a</sup>, Luis R. Lopes<sup>a,e</sup>, Perry M. Elliott<sup>a,e</sup>, Joaquim M.S. Cabral<sup>b,c</sup>, Maria Carmo-Fonseca<sup>d</sup>, Simão Teixeira da Rocha<sup>b,c,\*</sup>, Sandra Martins<sup>d,\*</sup>

<sup>a</sup> University College London Institute of Cardiovascular Science, Rayne Institute, 5 University Street, London WC1E 6JF, United Kingdom

<sup>b</sup> iBB – Institute for Bioengineering and Biosciences and Department of Bioengineering, Instituto Superior Técnico, Universidade de Lisboa, Av. Rovisco Pais, 1049-001 Lisboa, Portugal

<sup>c</sup> Associate Laboratory i4HB Institute for Health and Bioeconomy, Instituto Superior Técnico, Universidade de Lisboa, Av. Rovisco Pais, 1049-001 Lisboa, Portugal

<sup>d</sup> Fundação GIMM - Gulbenkian Institute for Molecular Medicine, Avenida Professor Egas Moniz, 1649-028 Lisboa, Portugal

<sup>e</sup> Barts Heart Centre, St. Bartholomew's Hospital, W Smithfield, EC1A 7BE London, United Kingdom

### ARTICLE INFO

#### Keywords:

iPSC  
Non-canonical splicing variants  
MYBPC3  
Hypertrophic cardiomyopathy

### ABSTRACT

Hypertrophic cardiomyopathy (HCM) is the most prevalent inherited cardiomyopathy and a leading cause of sudden death. Genetic testing and familial cascade screening play a pivotal role in the clinical management of HCM patients. However, conventional genetic tests primarily focus on the detection of exonic and canonical splice site variation. Oversight of intronic non-canonical splicing variants potentially contributes to a proportion of HCM patients remaining genetically undiagnosed. Here, using a non-integrative reprogramming strategy, we generated induced pluripotent stem cell (iPSC) lines from four individuals carrying one of two variants within intronic regions of *MYBPC3*: c.1224-52G > A and c.1898-23A > G. Upon differentiation to iPSC-derived cardiomyocytes (iPSC-CMs), mis-spliced mRNAs were identified in cells harbouring these variants. Both abnormal mRNAs contained a premature termination codon (PTC), fitting the criteria for activation of nonsense mediated decay (NMD). However, the c.1898-23A > G transcripts escaped this mRNA quality control mechanism, while the c.1224-52G > A transcripts were degraded. The newly generated iPSC lines represent valuable tools for studying the functional consequences of intronic variation and for translational research aimed at reversing splicing abnormalities to prevent disease progression.

### 1. Introduction

Hypertrophic cardiomyopathy (HCM) is the most common inherited cardiomyopathy and a leading cause of sudden cardiac death (SCD) (Braunwald 2015; Semsarian et al., 2015). This condition is characterised by hypertrophy, myocardial fibrosis and diastolic dysfunction, and is associated with complications including thromboembolism and heart failure (Ho, 2009; Maron, 2004; Suay-Corredera et al., 2021).

Likely pathogenic/pathogenic variants in myosin heavy chain (*MYH7*) and myosin-binding protein C (*MYBPC3*) are together responsible for approximately half of all HCM genotype-positive cases (Marian

and Braunwald 2017). Genetic testing plays an important clinical role in improving diagnostic certainty to distinguish sarcomeric HCM from phenocopies, and to facilitate familial cascade screening to identify at-risk relatives (Bonaventura et al., 2021; Lopes et al., 2024). Nevertheless, the clinical impact of genetic testing is limited by a relatively low yield of positive results (~30–40%) and an incomplete understanding of genotype-phenotype associations (Richard et al., 2003; Elliott et al., 2014; Arbelo et al., 2023). One possible explanation for this is that mainly exonic and canonical splice site variations are considered clinically significant in the pathogenesis of HCM, while intronic variations are often disregarded. As intronic mutations may interfere with splicing

\* Corresponding authors at: iBB – Institute for Bioengineering and Biosciences and Department of Bioengineering, Instituto Superior Técnico, Universidade de Lisboa, Av. Rovisco Pais, 1049-001, Lisboa, Portugal (S.T. da Rocha) and Instituto de Medicina Molecular João Lobo Antunes, Faculdade de Medicina da Universidade de Lisboa, Avenida Professor Egas Moniz, 1649-028 Lisboa, Portugal (S.Martins).

E-mail addresses: [simao.rocha@tecnico.ulisboa.pt](mailto:simao.rocha@tecnico.ulisboa.pt) (S.T. da Rocha), [sandramartins@medicina.ulisboa.pt](mailto:sandramartins@medicina.ulisboa.pt) (S. Martins).

<sup>1</sup> These authors have contributed equally to the work.

(Vaz-Drago et al., 2017; Barbosa et al., 2023), leading to gene expression misregulation, sequencing entire disease-associated genes might be particularly important in patients where exome sequencing approaches failed to identify a disease-causing variant.

The study of the pathogenesis of HCM has suffered from the limited availability of myocardial tissue. Moreover, tissue obtained from myectomy or cardiac transplantation fails to represent the early stages of disease development (Li et al., 2022). As an alternative, the differentiation of iPSCs into cardiomyocytes (iPSC-CMs) is becoming commonly used as a model for unravelling the molecular and pathophysiological mechanisms of HCM, while providing a platform for drug testing and screening (Dababneh et al., 2023; Caudal et al., 2024), facilitating the identification of potential therapeutic compounds and the development of targeted interventions for individuals with HCM.

In this study, we created iPSCs from patients with HCM who harbour intronic variants in the *MYBPC3* gene. We confirmed that these variants cause splicing abnormalities when iPSCs were differentiated into cardiac cells. These patient-derived iPSC lines provide an important resource for studying the impact of non-canonical splice-altering variants and to conduct further translational research to correct splicing abnormalities in HCM.

## 2. Materials and Methods

### 2.1. Study participants

Four unrelated individuals were recruited from the Barts Heart Centre, St. Bartholomew's Hospital, London, UK. The study conforms to the declaration of Helsinki. All patients gave written informed consent and the study was approved by a) the National Health Service (NHS) Health Research Authority (HRA) Regional Ethics Committee (REC, London-Bromley, UK), and b) the Central and East London Clinical Research Network (CEL CLRN) – Barts Health Permission Centre (London, UK), Study title: Inherited Cardiac Disease: A clinical and genetic investigation; ref: 15/LO/0549 and 010534). Samples were obtained from patients with no known causal HCM variant on established gene panels and harbouring intronic *MYBPC3* variants predicted to alter splicing by SpliceAI (cryptic splice-altering variants) or LabBranchoR (branchpoint disruption variants) (Lopes et al., 2020). The demographic and clinical characteristics of these patients are summarised in Table 1.

### 2.2. Sample collection

Whole blood was collected by regular venepuncture in BD Vacutainer® CPT™ tubes (BD Biosciences, #362761). Peripheral blood mononuclear cells (PBMCs) were isolated from whole blood using Ficoll™ Hypaque™ Solution, according to the Institute of Molecular Medicine (IMM) biobank, Lisbon, Standard Operating Procedure (SOP) protocol, and cryopreserved in 20 % DMSO (Merck, #D8418) in foetal bovine serum (FBS) (Life Technologies, #10500).

### 2.3. Generation of human induced pluripotent stem cells

For reprogramming, PBMCs were thawed and cultured in StemPro™-34 medium (Gibco #10639011), with the appropriate cytokines (IL-3, IL-6, FLT-3 and SCF –Preprotech/Tebu-bio, #200.03, 200.06, 300–19, 300–07, respectively) for 4 days. Cells were then plated at a density of  $5 \times 10^5$  cells/ml and transduced using CytoTune™-iPS 2.0 Sendai (SeV) Reprogramming Kit (Thermo Fisher Scientific, #A16517), according to the manufacturers' instructions. At day 3 post transduction, cells were reseeded into 9.5 cm<sup>2</sup> culture dishes coated with Matrigel™ (Corning, #354230) and cultured in mTeSR™ Plus (mTeSR +) Medium (STEMCELL Technologies, #100–0276). Based on stem cell morphology, colonies were individually picked and transferred to new Matrigel coated-plates in the first 5 passages. Cells were then passaged when the colonies covered ~ 80 % of the surface area of the culture dish approximately

**Table 1**

Clinical characterization of HCM participants enrolled in this study.

Patient Identifier	Mutation	Sex	Age at recruitment	Diagnosis and clinical interventions
H17	<i>MYBPC3</i> c.1224-52G > A	Female	23 years	Asymmetric septal HCM, with maximal wall thickness (MWT) of 29 mm. Patient was referred for an implantable cardioverter defibrillator (ICD) and for transplant assessment.
H22	<i>MYBPC3</i> c.1224-52G > A	Female	56 years	Asymmetric septal HCM, with MWT of 24 mm. Patient has ICD for primary prevention.
H24	<i>MYBPC3</i> c.1898-23A > G	Female	43 years	Subclinical HCM, with MWT of 12 mm in the septum. Patient showed non-sustained ventricular tachycardia (NSVT) and syncope and was implanted with a subcutaneous ICD.
H35	<i>MYBPC3</i> c.1898-23A > G	Female	58 years	Asymmetric septal HCM, with MWT of 16 mm. Patient had alcohol septal ablation and secondary prevention ICD following out-of-hospital ventricular fibrillation arrest (OOHVFA).

every 2–3 days, using 0.5 mM EDTA dissociation buffer (ThermoFisher Scientific, #15575020). Medium was changed every two days. Cells were continuously passaged and from passage 10 were constantly monitored for SeV clearance by qRT-PCR (see below). All the experiments documented here were performed on SeV-free iPSCs, in an incubator at 37 °C and 5 % CO<sub>2</sub> in normoxia conditions. iPSCs were confirmed to be mycoplasma free using qPCR Mycoplasma Test (MycoplasmaCheck, Eurofins Genomics) in accordance with the manufacturer's instructions.

### 2.4. Cardiac differentiation

iPSCs were plated at a density of  $9 \times 10^5$  cells in Aggrewell™ 800 plates (STEMCELL Technologies, #34815) in mTeSR + and ROCK inhibitor (ROCKi) (STEMCELL Technologies, #72304). Media changes were performed for the following 2 days for mTeSR + without ROCKi. Three days after plating, the medium was changed to RPMI 1640 (ThermoFisher Scientific #21875034) + B27-Ins 2 % (ThermoFisher Scientific #A1895601) supplemented with 11 μM CHIR (STEMCELL Technologies #72052) to induce mesoderm commitment. After 24 h, medium was replaced to RPMI 1640 + B27-Ins 2 % and kept until day 3 post-mesoderm commitment, where aggregates were supplemented with 5 μM IWP-4 (STEMCELL Technologies #72552) to induce cardiac lineage commitment. At day 7 post-mesoderm commitment, aggregates were transferred to ultra-low attachment plates (Corning #3471) and cultured with RPMI-1640 + B27 (2 %). Media was changed each two days and on day 13 of differentiation, iPSC-CMs were collected for further analysis. To inhibit NMD, iPSC-CMs at day 13 of differentiation were incubated with 5 μg/ml cycloheximide (Sigma, C7698) for 6 h.

2.5. G-banding karyotype

iPSCs were treated with 10 µg/ml colcemid (ThermoFisher Scientific, #15212012) for 5 h at 37 °C to arrest cells in metaphase. Cells were then harvested following incubation with Accutase (STEMCELL Technologies, #07922) for 7 min at 37 °C and further incubated with a hypotonic potassium chloride solution (pre-warmed at 37 °C) for 30 min at 37 °C. Finally, cells were fixed with 1:3 (v/v) acetic acid: methanol solution. Karyotype analysis was performed by Genomed SA (Lisbon, Portugal). More than 20 independent metaphase spreads were counted per cell line.

2.6. Flow cytometry

iPSC colonies were dissociated to single cells using Accutase, which were fixed in 2 % paraformaldehyde (PFA) for 15 min and then stored at 4 °C until use. For surface staining (SSEA4 and TRA1-60 antibodies) (Table 2), cells were resuspended in conjugated primary antibody diluted in 3 % bovine serum albumin (BSA) in phosphate buffered saline (PBS) solution (3 % FBS/1x PBS), for 30 min at room temperature (RT). For intracellular staining (OCT4 and SOX2 antibodies) (Table 2), cells were resuspended in 3 % FBS/1x PBS, centrifuged at 1200 x g for 3 min, and then permeabilized with 0.1 % Saponin (Sigma, #SAE0073) for 15

min at RT. Cells were then washed twice with 1 % FBS/1x PBS and incubated with primary antibodies diluted in 3 % FBS/1x PBS for 1 h at RT. Next, cells were washed twice with 1 % FBS/1xPBS and further incubated for 45 min, in the dark, with the secondary antibody (in 3 % FBS/1xPBS). Prior to analysis on FACSCalibur™ flow cytometer (Becton Dickinson), all cells were resuspended in 1x PBS. For each experimental sample, 10,000 events were collected within the defined gate, based on side scatter (SSC) and forward scatter (FSC). Results were analysed using FlowJo software.

2.7. Trilineage differentiation potential

Differentiation potential of iPSCs into the three germ layers was evaluated using STEMdiff Trilineage Differentiation Kit (STEMCELL Technologies, #05230). Briefly, cells were plated on Matrigel-coated coverslips and cultured in endoderm or mesoderm differentiation medium for 5 days, and ectoderm differentiation medium for 7 days. Cells in the coverslips were then fixed by incubation with 3.7 % PFA/1x PBS for 15 min at RT or collected for RNA extraction and analysed by immunofluorescence or qRT-PCR, respectively.

**Table 2**  
Antibodies and primers used in this study.

Antibodies used for immunocytochemistry/flow-cytometry				
	Antibody	Dilution	Company Cat #	RRID
Pluripotency Markers (Flow Cytometry and Immunofluorescence)	Mouse anti-OCT4	1:200	Millipore, MAB4419	AB_1977399
	Mouse anti-SOX2	1:200	R&D Systems, MAB2018	AB_358009
	Mouse anti-SSEA4 (PE)	1:20	Miltenyi Biotec, 130-098-369	AB_2653519
	Mouse anti-TRA1-60 (PE)	1:10	Miltenyi Biotec, 130-100-347	AB_2654227
Differentiation Markers (Immunofluorescence)	Rabbit anti-PAX6	1:400	Biologend, 901301	AB_2565003
	Mouse anti-NESTIN	1:400	R&D Systems, MAB2736	AB_2282664
	Rabbit anti-SOX17	1:200	Abcam, ab224637	AB_2801385
	PE Mouse anti-CD184	1:20	Biologend, 306506	AB_314612
	Mouse anti-αSMA	1:100	SIGMA, A2547	AB_476701
Cardiac Markers (Immunofluorescence and Immunoblotting)	Mouse anti-Troponin T (13-11) (cTnT)	1:500	Invitrogen, MA5-12960	AB_11000742
	Mouse anti-MYBPC3 (F-1)(c-MyBP-C)	1:500	Santa Cruz Biotechnology, sc-137181	AB_2017318
Others(Immunoblotting)	Mouse anti-GAPDH (0411)	1:3000	Santa Cruz Biotechnology, sc-47724	AB_627678
Secondary antibodies (Flow Cytometry)	Goat anti-mouse IgG, Alexa Fluor 488	1:1000	Thermo Fisher Scientific, A-11001	AB_2534069
Secondary antibodies (Immunofluorescence)	Goat anti-mouse IgG, Alexa Fluor 546	1:500	Thermo Fisher Scientific A-11003	AB_2534071
	Goat anti-mouse IgG, Alexa Fluor 488	1:500	Thermo Fisher Scientific, A-11001	AB_2534069
	Goat anti-rabbit IgG, Alexa Fluor 488	1:500	Thermo Fisher Scientific A-11034	AB_2576217
Secondary antibodies (Immunoblotting)	Goat anti-mouse IgG (H + L)-HRP conjugate	1:3000	Bio-Rad, 1706516	AB_11125547
Primers				
	Target	Size of amplicon	Forward/Reverse primer (5'-3')	
Sendai reprogramming vector (qRT-PCR)	SeV	181	GGATCACTAGGTGATATCGAGC/ ACCAGACAAGAGTTTAAGAGATATGTATC	
House-Keeping Genes (qRT-PCR)	GAPDH	238	TCGTGGAGTCCACTGGCGTC/ TCATGAGTCCTCCACGATAC	
	U6	126	CGTTCGGCAGCACATATAC/AAATATGGAACGCTTCACGA	
Mesoderm and Cardiac Markers (qRT-PCR)	Brachyury	102	TCAGCAAAGTCAAGCTCACCA/ CCCCAACTCTCACTATGTGGATT	
	MYBPC3	216	TAGCAAGAAGCCACGGTCAG/ CCAGCAATGACTGCGTAAGA	
	TNNT2	104	AGAGCGAAAAGTGGGAAGA/ GCTGATCTTCATTCAGGTGGT	
Targeted mutation analysis (RT-PCR)	MYBPC3 c.1224-52G > A	212 (WT)/262 (mut)	GGCATGCTAAAGAGGCTCAA/ GCACCGATGGACTCAAAGAT	
	MYBPC3 c.1898-23A > G	134 (WT)/239 (mut)	CCACAAACTGACCATTGACG/CCTGCCTGGGTACGAAGT	
Intron retention analysis (qRT-PCR)	MYBPC3 (intron 19)	136	CTGCAACCTGTGACCCAAGTGCAAGAGAAGGAAGAGCAAAG	
NMD efficiency analysis (qRT-PCR)	Firefly luciferase	236	ACATTAAGAAAAGGCCAGCGATTCTCGCTACACACCACGA	

## 2.8. Immunofluorescence

Cells plated on coverslips were fixed with 3.7 % PFA/1x PBS for 15 min at RT, permeabilized with 0.5 % Triton X-100 in 1x PBS (Sigma) for 10 min at RT, and blocked with 5 % FBS in PBS for 30 min at RT. Primary antibodies for the indicated proteins (Table 2) diluted in blocking solution were added to coverslips for overnight incubation at 4 °C. The following day, secondary antibodies (Table 2) diluted in 1 % FBS in 1x PBS were added for 1 h at RT. After nuclear counterstaining with 4',6-diamidino-2-phenyl-indole (DAPI, 0.2 mg/ml; Sigma, #D9542), coverslips were mounted in Mowiol (Sigma), and fluorescent images were acquired using Zeiss LSM 710 Confocal Laser Point-Scanning Microscope.

## 2.9. RNA extraction and qRT-PCR

Total RNA was extracted using NZYol (NZYTech®, MB18501) with a standard protocol, and contaminating DNA was removed by DNase I (Roche®, 04716728001) treatment. Complementary cDNA synthesis was achieved with the Transcriptor High Fidelity cDNA Synthesis Kit (Roche®, 5081963001). For validation of Sendai reprogramming vector clearance, the presence of viral transgenes (SeV) was detected by qRT-PCR, using specific primers (Table 2) and iTaq Universal SyBr Green Supermix (Bio-Rad, 1725274) in ViiA 7 Real-Time PCR System (Applied Biosystems). Mesoderm and cardiac commitment were assessed using specific primers (Table 2) for *BRACHYURY* or *MYBPC3* and *TNNT2*. mRNA expression levels are presented as the fold change of the target gene expression upon normalisation against the *GAPDH* or *U6* house-keeping snRNA ( $2^{-\Delta Ct}$ ). For splicing assays, RNA was extracted as described above and the presence of mutant mRNA was evaluated by RT-PCR using *MYBPC3* exonic primers flanking the intronic variants (Table 2 and Fig. 4A, B). Wild-type (WT) and mutant *MYBPC3* levels were further assessed by qRT-PCR using Universal SYBR Green Supermix (Bio-Rad).

## 2.10. Immunoblotting

Whole-cell lysates were prepared by resuspending aggregates into SDS-PAGE buffer (62.5 mM Tris-HCl, pH 6.8, 2 % SDS, 5 %  $\beta$ -mercaptoethanol, 10 % glycerol, 0.01 % bromophenol blue) with 200 U/ml benzonase (Sigma- Aldrich), incubating for 10 min at room temperature (RT), and then boiling for 5 min. For Western blot analysis, total protein extracts were separated on 10 % SDS-polyacrylamide gels and transferred to nitrocellulose membranes. Primary antibodies (Table 2) were diluted in blocking solution and incubated for 2 h at room temperature (RT). Horseradish peroxidase-coupled secondary antibodies (Table 2) diluted in 1x PBST were incubated for 1 h at RT, and detected by enhanced chemiluminescence (Amersham).

## 2.11. Nonsense-mediated mRNA decay (NMD) activity assay

On day 13 of differentiation, beating aggregates of iPSC-CMs were rinsed with 1xPBS, dissociated to single cells using 0,25 % Trypsin EDTA for 3 min at 37 °C, and resuspended in RPMI-1640 + B27 (2 %) medium at a density of  $4 \times 10^5$  cells/ml. The cells were then transfected with 500 ng of a PTC containing firefly luciferase plasmid (Carrard et al., 2023), using the STEM Lipo reagent (Invitrogen). Upon plating onto Matrigel-coated 12-well plates, an additional 500  $\mu$ l of 2x RPMI-1640 + B27 (2 %) were added to each well. 24 h after transfection, iPSC-CMs were collected for further RNA extraction in PureZOL® (Bio-Rad) reagent.

## 2.12. Statistical analysis

All statistical analyses were conducted using Prim8 software. To compare the means between two independent groups, unpaired t-tests were performed. Statistical significance was determined at a threshold

of  $p < 0.05$ . All results are presented as mean  $\pm$  standard error of the mean (SEM).

## 3. Results

### 3.1. Generation of patient-derived iPSC lines carrying *MYBPC3* intronic mutations

A cohort of individuals with a clinical diagnosis of HCM, but without an identified HCM-causing variant by conventional genetic screening panels, underwent targeted next generation sequencing (NGS) of 41 cardiomyopathy-associated genes or whole exome sequencing (WES) including a  $\sim 100$  bp intronic region beyond intron–exon boundaries (Lopes et al, 2020). From this cohort, four unrelated individuals harbouring likely pathogenic *MYBPC3* intronic variants, in heterozygosity, were selected based on high SpliceAI (Jaganathan et al., 2019) (threshold  $\geq 0.9$ ) or LabBranchoR scores: two of them carried the *MYBPC3* c.1224-52G > A variant, and the other two harboured the *MYBPC3* c.1898-23A > G variant (Fig. 1 and Table 1). The selection of four female individuals was incidental. Our previous study identified 29 patients carrying one of these variants, 18 of whom were male and 11 were female (Lopes et al., 2020).

Peripheral blood mononuclear cells (PBMCs) from the whole blood of each individual were isolated and then reprogrammed into iPSCs (Fig. 2A). Genomic DNA from iPSC clones (3\_H24 and 6\_H35 for *MYBPC3* c.1898-23A > G, and 4\_H17 and 4\_H22 for *MYBPC3* c.1224-52G > A) was extracted and submitted to Sanger sequencing. The presence of the *MYBPC3* variants, in heterozygosity, was confirmed in all selected clones (Fig. 1 and Fig. S1D). All the established iPSCs showed a typical stem-like morphology and stained positive for the pluripotent stem cell markers, OCT4 and SOX2, by immunofluorescence (IF) (Fig. 2B and Fig. S1A). Using flow cytometry, we quantitatively validated the expression of OCT4 and SOX2, and pluripotent surface markers TRA-1-60 and SSEA4 in all 4 iPSC clones (Fig. 2C and Fig. S1B).

Clonal identity was confirmed using short tandem repeat (STR) DNA analysis of parental PBMCs and derived iPSCs, with all 4 iPSC lines showing a normal female 46 XX karyotype (Fig. 2D and Fig. S1C). We also confirmed the iPSCs' capacity to differentiate into three lineages by using the STEMdiff™ trilineage differentiation kit and examining differentiation markers by IF and qRT-PCR. All 4 cell lines correctly differentiated into endoderm (IF staining for SOX17 and CD184), mesoderm (IF staining for  $\alpha$ SMA and positive for *BRACHYURY* by qRT-PCR) and ectoderm (IF staining for PAX6 and NESTIN) (Fig. S2A-D). These lines were registered in the Human Pluripotency Stem Cell Registry (<https://hpscereg.eu/>) under the names IBBISTi10-A for 4\_H17, IBBISTi11-A for 3\_H24, IBBISTi12-A for 6\_H35 and IBBISTi13-A for 4\_H22.

### 3.2. iPSC-CMs carrying intronic *MYBPC3* mutations exhibit abnormal splicing

Both *MYBPC3* c.1224-52G > A and *MYBPC3* c.1898-23A > G variants have been previously shown to alter splicing (Bagnall et al, 2018; Lopes et al, 2020; Holliday et al, 2021). However, while, in the case of the *MYBPC3* c.1224-52G > A variant, splicing changes were reported in patient PBMCs (Bagnall et al, 2018) and further validated in patient-derived iPSC-CMs (Holliday et al, 2021), for the *MYBPC3* c.1898-23A > G variant, such changes were only identified in patient PBMCs and required further validation in cardiac cells (Lopes et al, 2020). Interestingly, the impact of these two variants, at the RNA level, is predicted by bioinformatic algorithms (SpliceAI) to be distinct. The c.1224-52G > A variant creates a cryptic splice site, resulting in a 50 bp extension of exon 14. This leads to a frameshift and a premature stop codon (PTC), likely triggering nonsense-mediated mRNA decay (NMD). The c.1898-23A > G variant is predicted to disrupt the branchpoint in intron 19, causing full intron retention and the introduction of a PTC, which should

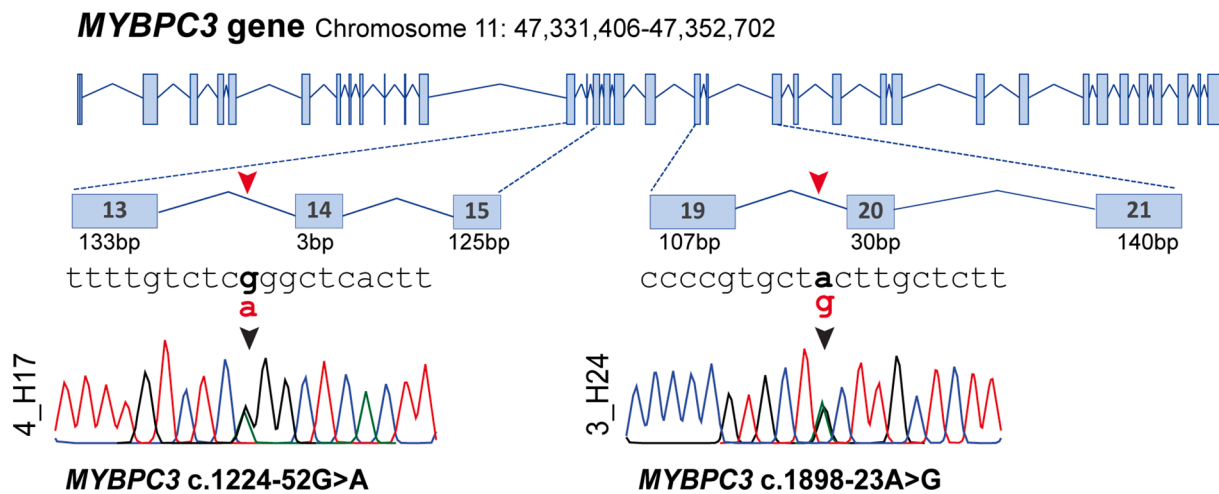


Fig. 1. Schematic representation of *MYBPC3* showing Sanger sequencing of the regions where the c.1224-52G > A and c.1898-23A > G variants are located.

also prompt NMD-mediated degradation of the mutant transcripts. To confirm missplicing of *MYBPC3* transcripts and NMD activation in the generated cell lines, a control (WT) iPSC derived from a healthy individual (Silva et al., 2020) and patient-derived iPSC lines were differentiated into iPSC-CMs (Branco et al., 2019) (Fig. 3A). Both control and patient-derived cells began spontaneously contracting starting on day 7 of the differentiation process. On day 13, *TNNT2* and *MYBPC3* expression in control iPSC-CMs was detected by qRT-PCR (Fig. 3B) and immunofluorescence (Fig. 3C), revealing the presence of sarcomeres with their characteristic striations.

We then analysed the splicing pattern of the exons adjacent to the introns where the *MYBPC3* variants were located. To prevent the potential degradation of abnormally spliced transcripts containing PTCs, iPSC-CMs were incubated with cycloheximide (CHX), a translation elongation inhibitor that is commonly used to suppress NMD (Miao et al., 2023). RT-PCR analysis of *MYBPC3* mRNAs from control (WT) and mutant iPSC-CMs revealed an additional upper band in patient-derived cells (Fig. 4A and 4B). In iPSC-CMs harbouring the *MYBPC3* c.1224-52G > A variant, the intensity of the upper band increased after CHX treatment (Fig. 4A), suggesting that a substantial fraction of mutant mRNAs are targeted for degradation by NMD. In contrast, in iPSC-CMs carrying the *MYBPC3* c.1898-23A > G variant the intensity of the upper band was similar with and without treatment with CHX (Fig. 4B), suggesting that the mutant mRNAs escape NMD.

Next, RT-PCR products were analyzed by Sanger sequencing (Fig. 4A and 4B). The results confirmed that the lower molecular weight products correspond to the WT mRNAs. In the case of *MYBPC3* c.1224-52G > A variant, the higher molecular weight products correspond to a 50 bp extension of *MYBPC3* exon 14, while in the case of the *MYBPC3* c.1898-23A > G variant there is a total retention of *MYBPC3* intron 19 (Fig. 4A and 4B).

Notably, we observed a faint upper band corresponding to intron 19 retention in WT iPSC-CMs (Fig. 4B). The presence of a minor fraction (~2%) of *MYBPC3* mRNAs retaining intron 19 in WT cells was confirmed by qRT-PCR (Fig. S3A). In mutant cells, mis-spliced transcripts represented approximately 12 % of all *MYBPC3* mRNAs (Fig. S3A).

We were intrigued by the finding that mis-spliced transcripts retaining intron 19 escape NMD. To rule out the possibility that mutant iPSC-CMs are NMD deficient, we used a PTC containing firefly luciferase construct (Fig. S3B) that was previously described (Carrard et al., 2023). On day 13 of differentiation, iPSC-CMs were transfected with the luciferase plasmid and 24 h after transfection the cells were either non-treated or treated with CHX for 6 h (Fig. S3B). Quantification of luciferase RNA levels by qRT-PCR showed a significant increase induced

upon CHX treatment (Fig. S3C), indicating that the mutant cells maintain the ability of targeting PTC containing transcripts for NMD-mediated degradation.

To further evaluate the impact of the *MYBPC3* variants on total mRNA levels we performed qRT-PCR assays using primers against *MYBPC3* exon 2. Compared to WT cells, the total amount of *MYBPC3* mRNA is significantly reduced in iPSC-CMs containing the c.1224-52G > A variant (Fig. 4C). In iPSC-CMs containing the c.1898-23A > G variant the RNA levels were slightly lower than in WT cells but the difference was not significant (Fig. 4C). Immunofluorescence with antibodies to cMyBP-C and cTnT revealed sarcomeres with typical striations in both mutant iPSC-CMs (Fig. 4D). Western blot analysis showed lower levels of cMyBP-C specifically in cells with the c.1224-52G > A variant (Fig. 4E).

In conclusion, we found that the intronic *MYBPC3* variants interfere with splicing in iPSC-CMs, but the stability of the mis-spliced RNA and the levels of c-MyBP-C protein differ depending on the variant.

#### 4. Discussion

As a leading cause of SCD, the genetic basis of HCM has been widely studied. To date, several studies have suggested a role for intronic variation in causing or modifying the disease phenotype using prediction-based software and RNA analysis (Frisso et al., 2016; Bagnall et al., 2018; Singer et al., 2019; McNamara et al., 2020; Lopes et al., 2020; Wood et al., 2021; Holiday et al., 2021; Torrado et al., 2022), arguing for the importance of whole genome sequencing (WGS) in patients for whom conventional genetic testing has failed to identify the disease-causing variant.

Disease-causing variants in *MYBPC3* account for approximately 30–40 % of all mutations identified in HCM (Nie et al., 2023). The majority of these *MYBPC3* variants are nonsense, frameshift and canonical splice site mutations, which are expected to cause loss-of-function. Haploinsufficiency has therefore been proposed as the disease mechanism underlying most *MYBPC3* variants (Ito et al., 2017; Suay-Corredera et al., 2021), contrary to other HCM causal genes, namely *MYH7*, where missense variants prevail (Marian 2021).

As *MYBPC3* is robustly expressed only in the heart (Tudurachi et al., 2023), the limited availability of myocardial tissue has been a significant obstacle to study the impact of *MYBPC3* variants in HCM aetiology. In recent years, advancements in iPSC technology have enabled the creation of cellular models for studying cardiac diseases, greatly improving our understanding and investigation of variants of unknown significance (VUS) found in large patient cohorts (Funakoshi and Yoshida 2021; Huang et al., 2021). Whilst numerous studies have used iPSC-CMs

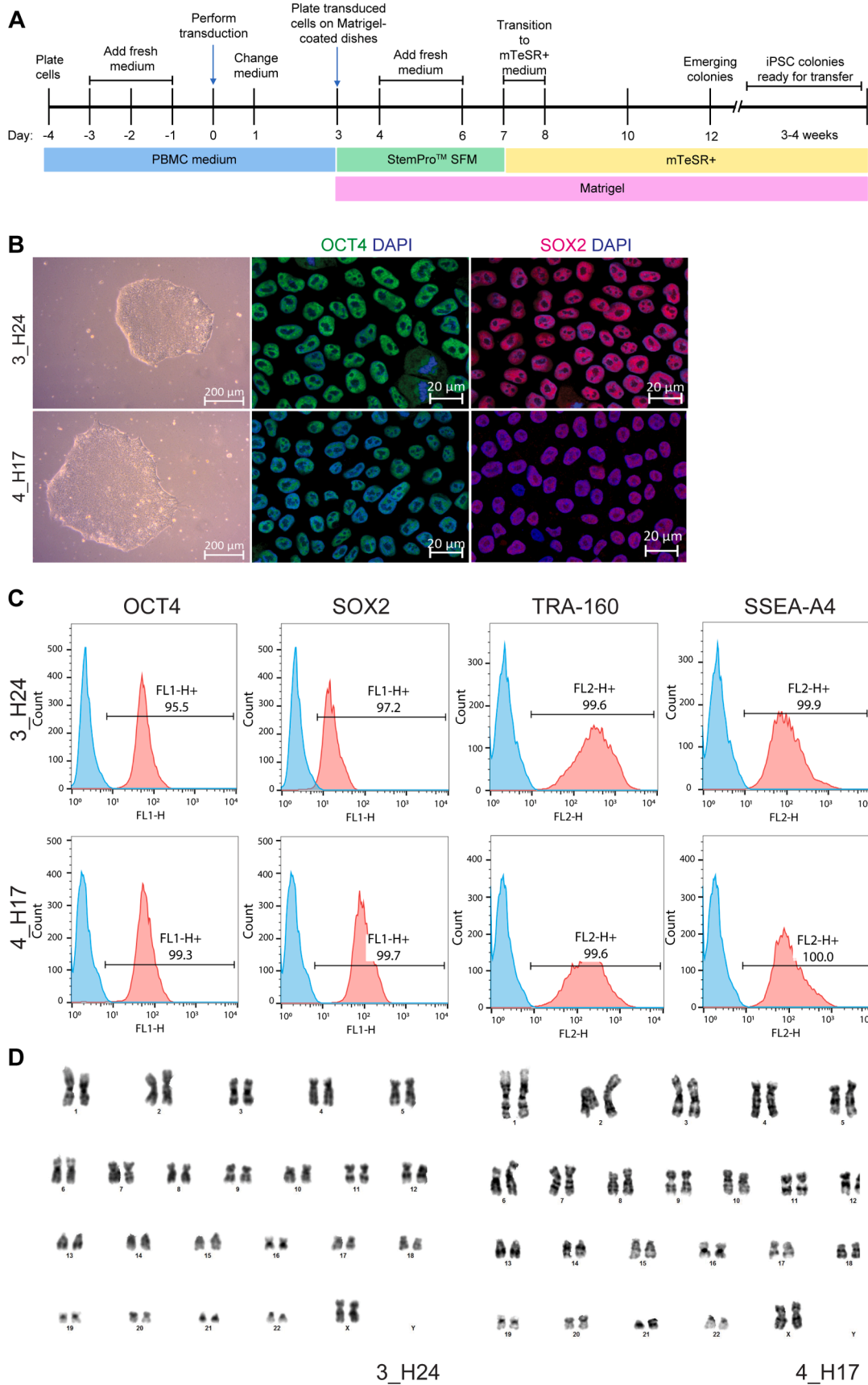


**Fig. 2.** Characterisation of the 3\_H24 and 4\_H17 iPSC lines. (A) Schematic of the Sendai virus reprogramming protocol of PBMCs to iPSCs. (B) On the left, bright field photomicrograph of iPSC colonies. Scale bar, 200  $\mu$ m. On the right, representative immunofluorescence images for OCT4 and SOX2 staining. Scale bar, 20  $\mu$ m. (C) Flow cytometry analysis of the indicated pluripotent stem cell markers. (D) G-banding karyotyping.

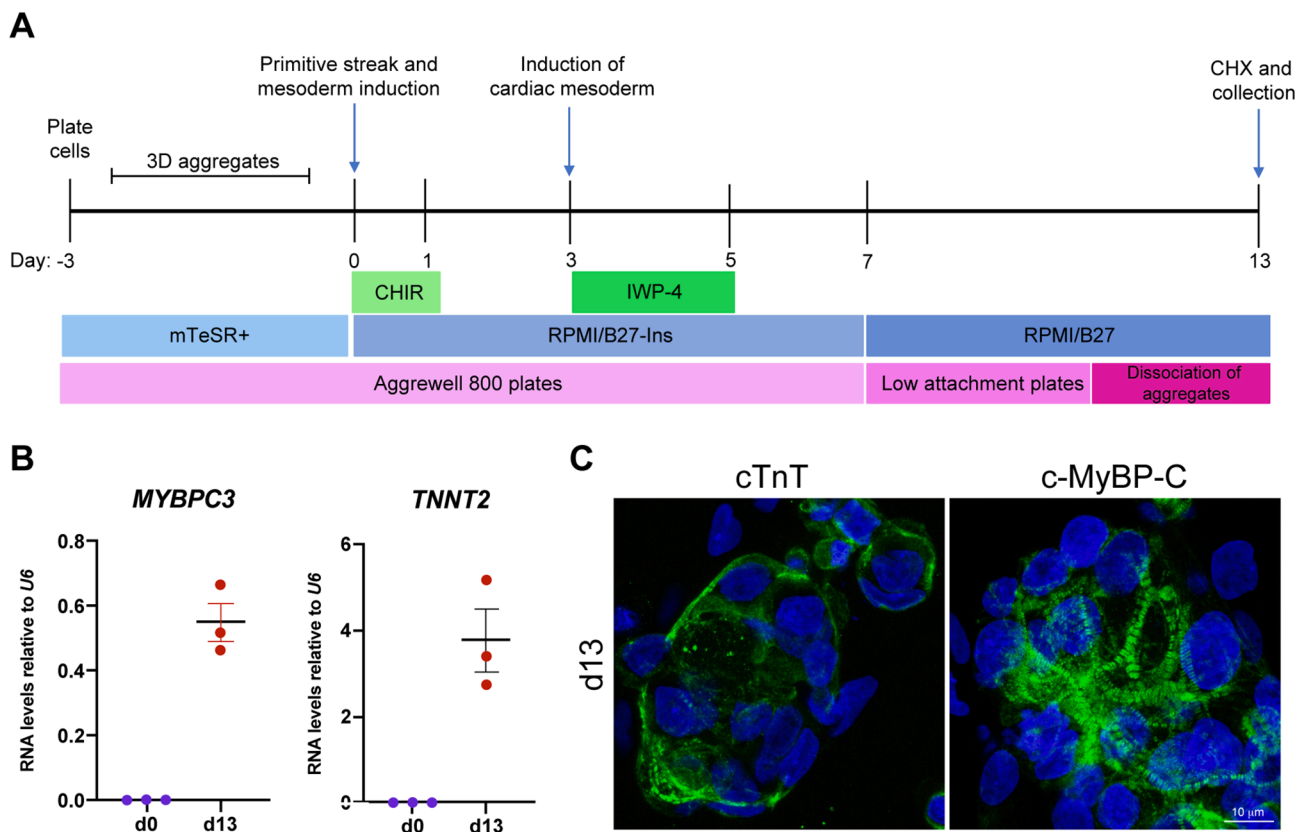


**Fig. 3.** Directed differentiation of iPSCs to cardiomyocytes. (A) Timeline and cell culture conditions used for differentiation. (B) qRT-PCR analysis of *MYBPC3* and *TNNT2* cardiac markers in iPSC-CMs derived from a healthy individual at day 0 (d0) and day 13 (d13) of differentiation. Graphs depict mRNA expression levels ( $2^{-\Delta\Delta Ct}$ ) relative to *U6* snRNA. Dots represent data from 3 independent differentiation experiments. The mean  $\pm$  SEM is depicted. (C) Immunofluorescence of iPSC-CMs derived from a healthy individual at day 13 of differentiation. Sarcomeric proteins c-MyBP-C and cTnT are stained in green. Nuclei stained with DAPI (in blue).

carrying *MYBPC3* variants as a tool for HCM disease modelling (Ojala et al., 2016; Seeger et al., 2019; Jin et al., 2020; Lui et al., 2021; Warnecke et al., 2021), few have focussed on studying the functional impact of intronic *MYBPC3* variants found in a subset of patients subjected to WGS (Singer et al., 2023).

In this work, we successfully generated and characterised four iPSC lines from PBMCs obtained from HCM patients harbouring one of two previously identified intronic *MYBPC3* variants. This was achieved using a non-integrative reprogramming approach with Sendai virus vectors to deliver the Yamanaka factors. Upon cardiac differentiation, we found that the c.1224-52G > A variant created a cryptic splice site upstream of the canonical 3' splice site, resulting in the extension of exon 14 by 50 nucleotides (Fig. 4A). Aberrantly spliced transcripts contain a PTC and are flagged for degradation by NMD (Fig. 4A). As a result, the levels of *MYBPC3* mRNA and cMyBP-C protein are reduced (Fig. 4C, E), suggesting a loss-of-function mechanism.

The *MYBPC3* c.1898-23A > G variant was previously shown to induce splicing alterations in PBMCs collected from HCM patients (Lopes et al., 2020). Although RNA extracted from PBMCs enables meaningful detection of mis-spliced *MYBPC3* transcripts in HCM patients, further validation in cardiac cells, where sarcomeric genes are robustly expressed and regulated, was lacking. This study addresses this gap by demonstrating splicing alterations in patient-derived iPSC-CMs at early stages of cardiac differentiation.

Splicing abnormalities associated with the *MYBPC3* c.1898-23A > G variant result in branchpoint disruption and full retention of intron 19 (Fig. 4B). This leads to introduction of a PTC upstream of the canonical splice site at intron 19. However, the mis-spliced transcripts are not degraded by NMD, despite containing a PCT that meets the minimum required distance of over 50 nucleotides from the next exon-exon

junction. When an exon junction complex (EJC) is deposited at this junction, it should trigger EJC-dependent degradation of the mis-spliced transcripts (Ishigaki et al., 2001). Understanding why these aberrant mRNAs escape NMD requires further investigation.

The total levels of *MYBPC3* mRNA and c-MyBP-C protein in iPSC-CMs harboring the c.1898-23A > G mutation are similar to those of control cells (Fig. 4C, E). In agreement with this finding, previous research has shown that there is not a consistent decrease in c-MyBP-C protein levels in cardiomyocytes with *MYBPC3* pathogenic variants (Helms et al. 2020). Specifically, it remains to be determined whether the mis-spliced mRNAs produced in iPSC-CMs harboring the c.1898-23A > G mutation result in the production of truncated c-MyBP-C with a dominant-negative effect.

In conclusion, taking advantage of iPSC technology, we have added evidence that intronic *MYBPC3* variants interfere with splicing, leading to aberrant mRNA transcripts. We further show that, depending on the variant, mis-splicing may or may not alter c-MyBP-C protein levels. These newly established iPSC lines provide valuable cellular models for elucidating the mechanisms by which non-canonical splicing variants cause HCM. Additionally, they offer potential for developing targeted therapeutic interventions tailored to individuals affected by this condition. Ultimately, this work highlights the importance of screening for intronic *MYBPC3* variants in the context of HCM, especially in patients with a family history of disease and where no exonic candidates had been previously identified by conventional gene panels and exome-sequencing approaches.

#### CRedit authorship contribution statement

Joanna Jager: Writing – original draft, Methodology, Investigation.

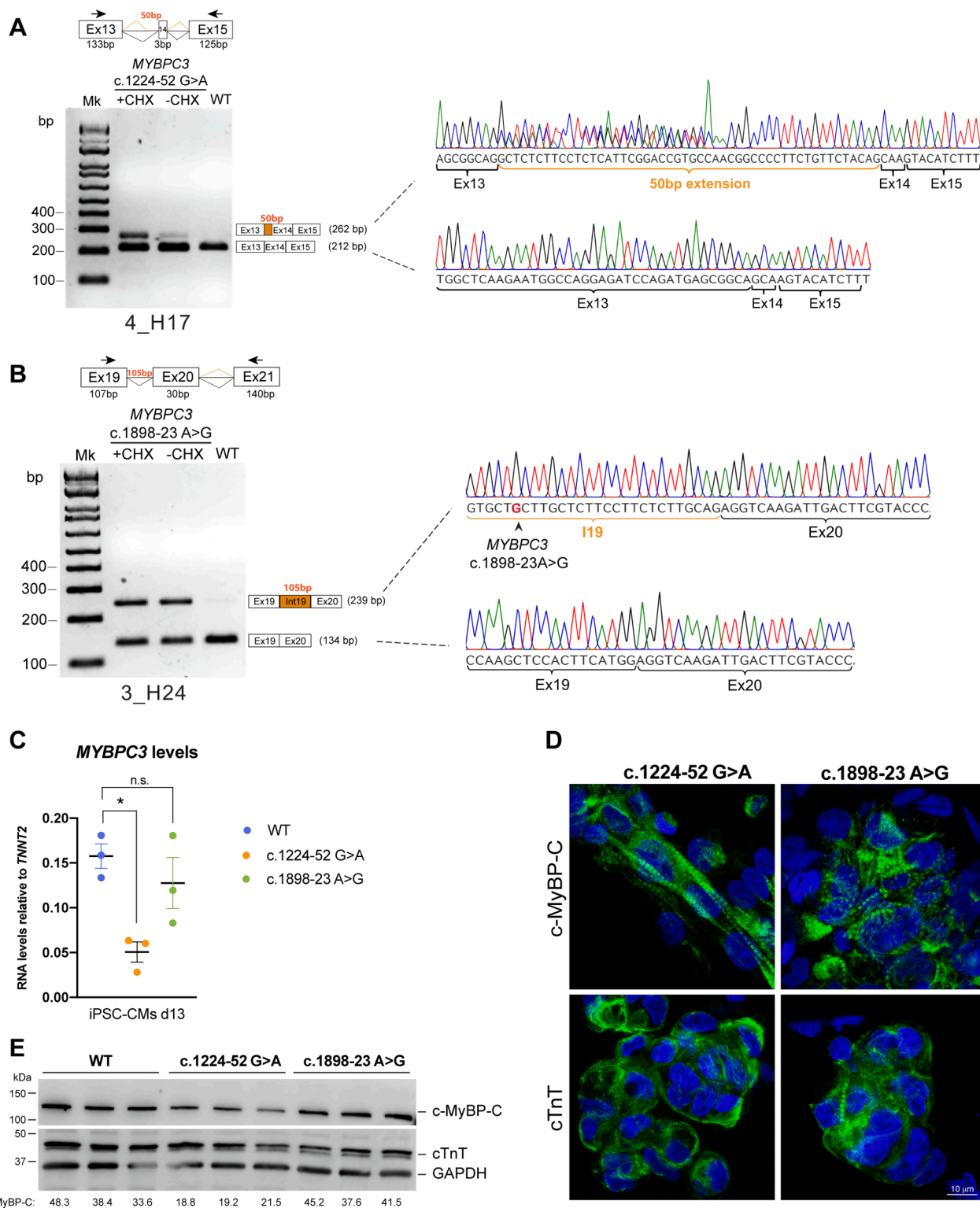


**Fig. 4.** Impact of the *MYBPC3* intronic variants on RNA and protein levels. (A, B) On the left, semi-quantitative RT-PCR analysis using the indicated primers (black arrows) in iPSC-CMs derived from a healthy individual (WT) and HCM patients with the c.1224-52G > A (A) and c.1898-23A > G (B) variants. Cells were either untreated (-CHX) or treated (+CHX) with cycloheximide for 6 h. Molecular size markers are indicated. On the right, Sanger sequencing of amplified RT-PCR products. (C) qRT-PCR analysis of *MYBPC3* mRNA relative to *TNN2* in the indicated iPSC-CMs at day 13 of differentiation. Dots represent data from 3 independent differentiation experiments. The mean  $\pm$  SEM is depicted. \*  $p < 0,05$ ; n.s. not significant. (D) Immunofluorescence of mutant iPSC-CMs at day 13 of differentiation. Sarcomeric proteins c-MyBP-C and cTnT are stained in green. Nuclei stained with DAPI (in blue). (E) Western blot analysis of the indicated iPSC-CMs at day 13 of differentiation. Molecular mass markers are indicated on the left. Quantification of the c-MyBP-C band intensity relative to cTnT is shown, in percentage, below. Data from 3 independent differentiation experiments.

**Marta Ribeiro:** Writing – original draft, Methodology, Investigation. **Marta Furtado:** Writing – original draft, Methodology, Investigation. **Teresa Carvalho:** Writing – review & editing, Methodology, Investigation. **Petros Syrris:** Writing – review & editing, Supervision, Methodology, Conceptualization. **Luis R. Lopes:** Writing – review & editing, Supervision, Methodology, Conceptualization. **Perry M. Elliott:** Writing – review & editing, Funding acquisition, Conceptualization. **Joaquim M.S. Cabral:** Writing – review & editing, Funding acquisition. **Maria Carmo-Fonseca:** Writing – review & editing, Supervision, Project administration, Methodology, Funding acquisition, Conceptualization. **Simão Teixeira da Rocha:** Writing – review & editing, Supervision, Project administration, Methodology, Investigation, Conceptualization. **Sandra Martins:** Writing – review & editing, Supervision, Project administration, Methodology, Investigation, Formal analysis, Conceptualization.

## Funding

This work was funded by a British Heart Foundation project grant (PG/20/10170), by “laCaixa” Foundation under the agreement LCF/PR/HR20/52400021 and by a grant from the Leducq Foundation for Cardiovascular Research (#21CVD02). J.J. was funded by the British Heart Foundation grant (PG/20/10170). L.R.L. was supported by a Medical Research Council UK Research and Innovation Clinical Academic Research Partnership award (MR/T005181/1). S.T. da R. was supported by an assistant research contract 2021.00660.CEECIND from Fundação para Ciência e Tecnologia/Ministério da Ciência, Tecnologia e Ensino Superior (FCT/MCTES). Further support was received from Fundação para a Ciência e Tecnologia (FCT), Portugal (Fellowship 2020.04836.BD to M.F.).

## Declaration of competing interest

The authors declare the following financial interests/personal relationships which may be considered as potential competing interests: M.C.-F. is a co-founder and advisor for “GenoMed-Diagnósticos de Medicina Molecular, SA”; she reports research support by AbbVie and Gilead Sciences, outside of the scope of this study; she also received speaker fees from Novartis, Janssen, AstraZeneca and Alnylam. L.R.L. speaker fee Alnylam, Sanofi-Genzyme and BMS and consulting fees BMS and Novo Nordisk. Research grant from BMS. The remaining authors have nothing to disclose. If there are other authors, they declare that they have no known competing financial interests or personal relationships that could have appeared to influence the work reported in this paper.

## Acknowledgments

We are grateful to the four individuals for their generous gift of a blood sample and to Ângela Afonso and her team from Biobanco-iMM for the PBMC collection. We are also thankful to Dr Fabrice Lejeune from CNRS, Inserm, University of Lille, France for kindly providing the vector carrying the cDNA coding for firefly luciferase.

## Appendix A. Supplementary data

Supplementary data to this article can be found online at <https://doi.org/10.1016/j.scr.2024.103582>.

## Data availability

Data will be made available on request.

## References

- Arbelo, E., Protonotarios, A., Gimeno, J.R., Arbustini, E., et al., 2023. ESC Guidelines for the management of cardiomyopathies. *Eur. Heart J.* <https://doi.org/10.1093/eurheartj/ehad194>.
- Bagnall, R.D., Ingles, J., Dinger, M.E., Cowley, M.J., Ross, S.B., Minoche, A.E., Lal, S., Turner, C., Colley, A., Rajagopalan, S., Berman, Y., Ronan, A., Fatkin, D., Semsarian, C., 2018. Whole Genome Sequencing Improves Outcomes of Genetic Testing in Patients With Hypertrophic Cardiomyopathy. *J Am Coll Cardiol.* <https://doi.org/10.1016/j.jacc.2018.04.078>.
- Barbosa, P., Savaiaar, R., Carmo-Fonseca, M., Fonseca, A., 2023. Computational prediction of human deep intronic variation. *GigaScience.* <https://doi.org/10.1093/gigascience/giad085>.
- Bonaventura, J., Polakova, E., Vejtasova, V., Veselka, J., 2021. Genetic Testing in Patients with Hypertrophic Cardiomyopathy. *Int J Mol Sci.* <https://doi.org/10.3390/ijms221910401>.
- Branco MA, Cotovio JP, Rodrigues CAV, Vaz SH, Fernandes TG, Moreira LM, Cabral JMS, Diogo MM. Transcriptomic analysis of 3D Cardiac Differentiation of Human Induced Pluripotent Stem Cells Reveals Faster Cardiomyocyte Maturation Compared to 2D Culture (2019) *Sci Rep.* <https://doi.org/10.1038/s41598-019-45047-9>.
- Braunwald, E., 2015. Hypertrophic cardiomyopathy: The past, the present, and the future. In: Naidu, S.S. (Ed.), *Hypertrophic Cardiomyopathy*. Springer-Verlag; London, UK, pp. 1–8.
- Carrard, J., Rajaczak, F., Elsens, J., Leroy, C., Kong, R., Geoffroy, L., Comte, A., Fournet, G., Joseph, B., Li, X., Moebis-Sanchez, S., Lejeune, F., 2023. Identifying Potent Nonsense-Mediated mRNA Decay Inhibitors with a Novel Screening System. *Biomedicines.* <https://doi.org/10.3390/biomedicines11102801>.
- Caudal, A., Snyder, M.P., Wu, J.C., 2024. Harnessing human genetics and stem cells for precision cardiovascular medicine. *Cell Genom.* <https://doi.org/10.1016/j.xgen>.
- Dababneh, S., Hamledari, H., Maaref, Y., Jayousi, F., Baygi, D.H., Khan, A., Jannati, S., Jabbari, K., Arslanova, A., Butt, M., Roston, T.M., Sanatani, S., Tibbits, G.F., 2023. Advances in Hypertrophic Cardiomyopathy Disease Modeling using Human iPSC-derived Cardiomyocytes. *Can. J. Cardiol.* <https://doi.org/10.1016/j.cjca.2023.11.009>.
- Elliott, P.M., Anastasakis, A., Borger, M.A., Borggrefe, M., Cecchi, F., Charron, P., Hagege, A.A., Lafont, A., Limongelli, G., Mahrholdt, H., McKenna, W.J., Mogensen, J., Nihoyannopoulos, P., Nistri, S., Pieper, P.G., Pieske, B., Rapezzi, C., Rutten, F.H., Tillmanns, C., Watkins, H., 2014. 2014 ESC Guidelines on diagnosis and management of hypertrophic cardiomyopathy: the Task Force for the Diagnosis and Management of Hypertrophic Cardiomyopathy of the European Society of Cardiology (ESC). *Eur Heart J.* <https://doi.org/10.1093/eurheartj/ehu284>.
- Frisso, G., Datta, N., Coppola, P., Mazzaccara, C., Pricolo, M.R., D'Onofrio, A., Limongelli, G., Calabrò, R., Salvatore, F., 2016. Functional Studies and In Silico Analyses to Evaluate Non-Coding Variants in Inherited Cardiomyopathies. *Int J Mol Sci.* <https://doi.org/10.3390/ijms17111883>.
- Funakoshi, S., Yoshida, Y., 2021. Recent progress of iPSC technology in cardiac diseases. *Arch Toxicol.* <https://doi.org/10.1007/s00204-021-03172-3>.
- Helms, A.S., Tang, V.T., O'Leary, T.S., Friedline, S., Wauchope, M., Arora, A., Wasserman, A.H., Smith, E.D., Lee, L.M., Wen, X.W., Shavit, J.A., Liu, A.P., Previs, M.J., Day, S.M., 2020. Effects of MYBPC3 loss-of-function mutations preceding hypertrophic cardiomyopathy. *JCI Insight.* <https://doi.org/10.1172/jci.insight.133782>.
- Ho, C.Y., 2009. Hypertrophic cardiomyopathy: preclinical and early phenotype. *J Cardiovasc Transl Res.* <https://doi.org/10.1007/s12265-009-9124-7>.
- Holliday, M., Singer, E.S., Ross, S.B., Lim, S., Lal, S., Ingles, J., Semsarian, C., Bagnall, R.D., 2021. Transcriptome Sequencing of Patients With Hypertrophic Cardiomyopathy Reveals Novel Splice-Altering Variants in MYBPC3. *Circ Genom Precis Med.* <https://doi.org/10.1161/CIRCGEN.120.003202>.
- Huang, J., Feng, Q., Wang, L., Zhou, B., 2021. Human Pluripotent Stem Cell-Derived Cardiac Cells: Application in Disease Modeling, Cell Therapy, and Drug Discovery. *Front Cell Dev Biol.* <https://doi.org/10.3389/fcell.2021.655161>.
- Ishigaki, Y., Li, X., Serin, G., Maquat, L.E., 2001. Evidence for a pioneer round of mRNA translation: mRNAs subject to nonsense-mediated decay in mammalian cells are bound by CBP80 and CBP20. *Cell.* [https://doi.org/10.1016/s0092-8674\(01\)00475-5](https://doi.org/10.1016/s0092-8674(01)00475-5).
- Ito, K., Patel, P.N., Gorham, J.M., McDonough, B., DePalma, S.R., Adler, E.E., Lam, L., MacRae, C.A., Mohiuddin, S.M., Fatkin, D., Seidman, C.E., Seidman, J.G., 2017. Identification of pathogenic gene mutations in LMNA and MYBPC3 that alter RNA splicing. *Proc Natl Acad Sci USA.* <https://doi.org/10.1073/pnas.1707741114>.
- Jaganathan, K., Kyriazopoulou Panagiotopoulou, S., McRae, J.F., Darbandi, S.F., Knowles, D., Li, Y.I., Kosmicki, J.A., Arbelaez, J., Cui, W., Schwartz, G.B., Chow, E.D., Kanterakis, E., Gao, H., Kia, A., Batzoglu, S., Sanders, S.J., Farh, K.K., 2019. Predicting Splicing from Primary Sequence with Deep Learning. *Cell.* <https://doi.org/10.1016/j.cell.2018.12.015>.
- Jin J, Lu L, Chen J, Wang K, Han J, Xue S, Weng G. Generation of an induced pluripotent stem cell (iPSC) line from a patient with hypertrophic cardiomyopathy carrying myosin binding protein C (MYBPC3) c.3369-3370 insC mutation (2020) *Stem Cell Res.* doi: 10.1016/j.scr.2020.102144.
- Li, J., Feng, X., Wei, X., 2022. Modeling hypertrophic cardiomyopathy with human cardiomyocytes derived from induced pluripotent stem cells. *Stem Cell Res Ther.* <https://doi.org/10.1186/s13287-022-02905-0>.
- Liu, L., Shenoy, S.P., Jahng, J.W.S., Liu, Y., Knowles, J.W., Zhuge, Y., Wu, J.C., 2021. Generation of two heterozygous MYBPC3 mutation-carrying human iPSC lines, SCVli001-A and SCVli002-A, for modeling hypertrophic cardiomyopathy. *Stem Cell Res.* <https://doi.org/10.1016/j.scr.2021.102279>.

- Lopes, L.R., Barbosa, P., Torrado, M., Quinn, E., Merino, A., Ochoa, J.P., Jager, J., Futema, M., Carmo-Fonseca, M., Monserrat, L., Syrris, P., Elliott, P.M., 2020. Cryptic Splice-Altering Variants in *MYBPC3* Are a Prevalent Cause of Hypertrophic Cardiomyopathy. *Circ Genom Precis Med.* <https://doi.org/10.1161/CIRCGEN.120.002905>.
- Lopes, L.R., Ho, C.Y., Elliott, P.M., 2024. Genetics of hypertrophic cardiomyopathy: established and emerging implications for clinical practice. *Eur Heart J.* <https://doi.org/10.1093/eurheartj/ehae421>.
- Marian, A.J., Braunwald, E., 2017. Hypertrophic Cardiomyopathy: Genetics, Pathogenesis, Clinical Manifestations, Diagnosis, and Therapy. *Circ Res.* <https://doi.org/10.1161/CIRCRESAHA.117.311059>.
- Marian AJ (2021) Molecular Genetic Basis of Hypertrophic Cardiomyopathy. *Circ Res.* 2021 <https://doi.org/10.1161/CIRCRESAHA.121.318346>.
- Maron, B.J., 2004. Hypertrophic cardiomyopathy: an important global disease. *Am J Med.* <https://doi.org/10.1016/j.amjmed.2003.10.012>.
- McNamara, J.W., Schuckman, M., Becker, R.C., Sadayappan, S., 2020. A Novel Homozygous Intronic Variant in *TNNT2* Associates With Feline Cardiomyopathy. *Front Physiol.* <https://doi.org/10.3389/fphys.2020.608473>.
- Miao, Y., Du, Q., Zhang, H.G., Yuan, Y., Zuo, Y., Zheng, H., 2023. Cycloheximide (CHX) Chase Assay to Examine Protein Half-life. *Bio Protoc.* <https://doi.org/10.21769/BioProtoc.4690>.
- Nie, J., Han, Y., Jin, Z., Hang, W., Shu, H., Wen, Z., Ni, L., Wang, D.W., 2023. Homology-directed repair of an *MYBPC3* gene mutation in a rat model of hypertrophic cardiomyopathy. *Gene Ther.* <https://doi.org/10.1038/s41434-023-00384-3>.
- Ojala, M., Prajapati, C., Pölonen, R.P., Rajala, K., Pekkanen-Mattila, M., Rasku, J., Larsson, K., Aalto-Setälä, K., 2016. Mutation-Specific Phenotypes in hiPSC-Derived Cardiomyocytes Carrying Either Myosin-Binding Protein C Or  $\alpha$ -Tropomyosin Mutation for Hypertrophic Cardiomyopathy. *Stem Cells Int.* <https://doi.org/10.1155/2016/1684792>.
- Richard, P., Charron, P., Carrier, L., Ledeuil, C., Cheav, T., Pichereau, C., Benaiche, A., Isnard, R., Dubourg, O., Burban, M., Gueffat, J.P., Millaire, A., Desnos, M., Schwartz, K., Hainque, B., Komajda, M., 2003. EUROGENE Heart Failure Project. Hypertrophic cardiomyopathy: distribution of disease genes, spectrum of mutations, and implications for a molecular diagnosis strategy. *Circulation.* <https://doi.org/10.1161/01.CIR.0000066323.15244.54>.
- Seeger, T., Shrestha, R., Lam, C.K., Chen, C., McKeithan, W.L., Lau, E., Wnorowski, A., McMullen, G., Greenhaw, M., Lee, J., Oikonomopoulos, A., Lee, S., Yang, H., Mercola, M., Wheeler, M., Ashley, E.A., Yang, F., Karakikes, I., Wu, J.C., 2019. A Premature Termination Codon Mutation in *MYBPC3* Causes Hypertrophic Cardiomyopathy via Chronic Activation of Nonsense-Mediated Decay. *Circulation.* <https://doi.org/10.1161/CIRCULATIONAHA.118.034624>.
- Semsarian, C., Ingles, J., Maron, M.S., Maron, B.J., 2015. New perspectives on the prevalence of hypertrophic cardiomyopathy. *J Am Coll Cardiol.* <https://doi.org/10.1016/j.jacc.2015.01.019>.
- Silva, T.P., Bekman, E.P., Fernandes, T.G., Vaz, S.H., Rodrigues, C.A.V., Diogo, M.M., Cabral, J.M.S., Carmo-Fonseca, M., 2020. Maturation of Human Pluripotent Stem Cell-Derived Cerebellar Neurons in the Absence of Co-culture. *Front. Bioeng. Biotechnol.* <https://doi.org/10.3389/fbioe.2020.00070>.
- Singer, E.S., Ingles, J., Semsarian, C., Bagnall, R.D., 2019. Key Value of RNA Analysis of *MYBPC3* Splice-Site Variants in Hypertrophic Cardiomyopathy. *Circ Genom Precis Med.* <https://doi.org/10.1161/CIRCGEN.118.002368>.
- Singer, E.S., Crowe, J., Holliday, M., Isbister, J.C., Lal, S., Nowak, N., Yeates, L., Burns, C., Rajagopalan, S., Macciocca, I., King, I., Wacker, J., Ingles, J., Weintraub, R.G., Semsarian, C., Bagnall, R.D., 2023. The burden of splice-disrupting variants in inherited heart disease and unexplained sudden cardiac death. *NPJ Genom Med.* <https://doi.org/10.1038/s41525-023-00373-w>.
- Suay-Corredera C, Pricolo MR, Herrero-Galán E, Velázquez-Carreras D, Sánchez-Ortiz D, García-Giustiniani D, Delgado J, Galano-Frutos JJ, García-Cebollada H, Vilches S, Domínguez F, Molina MS, Barriales-Villa R, Frisso G, Sancho J, Serrano L, García-Pavía P, Monserrat L, Alegre-Cebollada J (2021) Protein haploinsufficiency drivers identify *MYBPC3* variants that cause hypertrophic cardiomyopathy. *J Biol Chem.* doi:10.1016/j.jbc.2021.100854.
- Torrado, M., Maneiro, E., Lamounier Junior, A., Fernández-Burriel, M., Sánchez Giralt, S., Martínez-Carapeto, A., Cazón, L., Santiago, E., Ochoa, J.P., McKenna, W.J., Santomé, L., Monserrat, L., 2022. Identification of an elusive spliceogenic *MYBPC3* variant in an otherwise genotype-negative hypertrophic cardiomyopathy pedigree. *Sci Rep.* <https://doi.org/10.1038/s41598-022-11159-y>.
- Tudurachi, B.S., Zăvoi, A., Leonte, A., Țăpoi, L., Ureche, C., Bîrgoan, S.G., Chiurariu, T., Anghel, L., Radu, R., Sascău, R.A., Stătescu, C., 2023. An Update on *MYBPC3* Gene Mutation in Hypertrophic Cardiomyopathy. *Int J Mol Sci.* <https://doi.org/10.3390/ijms241310510>.
- Vaz-Drago, R., Custódio, N., Carmo-Fonseca, M., 2017. Deep intronic mutations and human disease. *Hum Genet.* <https://doi.org/10.1007/s00439-017-1809-4>.
- Warnecke, N., Ulmer, B.M., Laufer, S.D., Shibamiya, A., Krämer, E., Neuber, C., Hanke, S., Behrens, C., Loos, M., Münch, J., Kühnisch, J., Klaassen, S., Eschenhagen, T., Patten-Hamel, M., Carrier, L., Mearini, G., 2021. Generation of bi-allelic *MYBPC3* truncating mutant and isogenic control from an iPSC line of a patient with hypertrophic cardiomyopathy. *Stem Cell Res.* <https://doi.org/10.1016/j.scr.2021.102489>.
- Wood, K.A., Ellingford, J.M., Eden, J., Thomas, H.B., O'Keefe, R.T., Hopton, C., Newman, W.G., 2021. Pathogenic Intronic Splice-Affecting Variants in *MYBPC3* in Three Patients with Hypertrophic Cardiomyopathy. *Cardiogenetics.* <https://doi.org/10.3390/cardiogenetics11020009>.